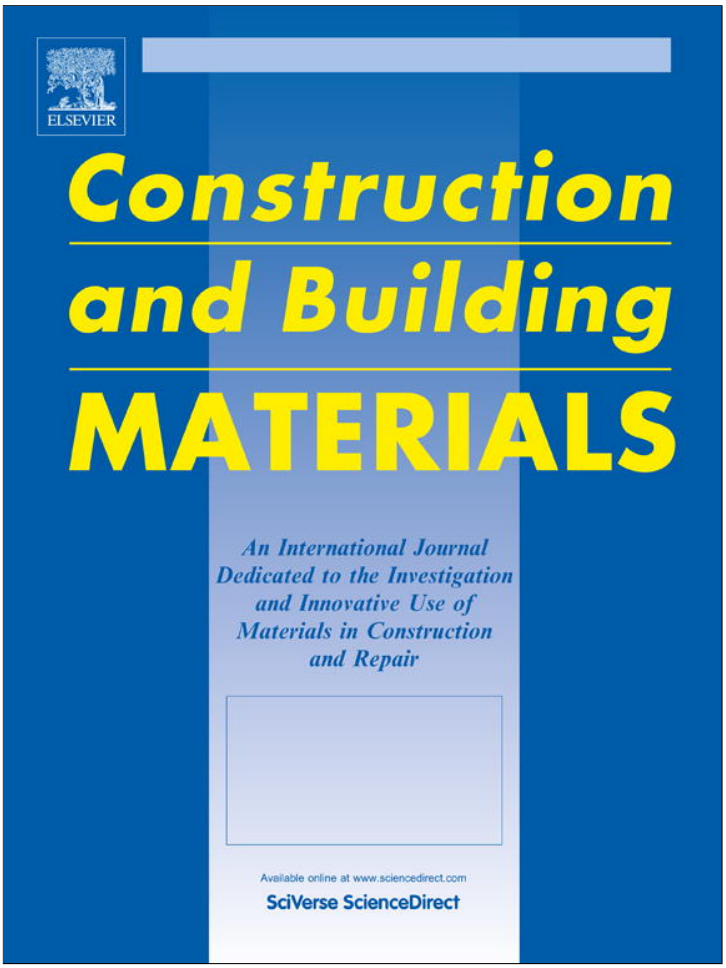

(This is a sample cover image for this issue. The actual cover is not yet available at this time.)

Construction and Building Materials 38 (2013) 139–146

Contents lists available at SciVerse ScienceDirect

Construction and Building Materials

journal homepage: www.elsevier.com/locate/conbuildmat

Chloride-induced corrosion of steel reinforcement – Mechanical performance and pit depth analysis

Charis A. Apostolopoulos [a], Sotiris Demis [b], Vagelis G. Papadakis [c,*]

[a] Department of Mechanical and Aeronautical Engineering, Laboratory of Technology and Strength of Materials, University of Patras, Patras 26500, Greece
[b] Department of Civil Engineering, University of Patras, Patras 26500, Greece
[c] Department of Environmental and Natural Resources Management, University of Western Greece, Seferi 2, Agrinio 30100, Greece

HIGHLIGHTS

- Effect of corrosion on bare B500c bars and embedded in concrete, under salt spray.
- Moderate loss of strength but significant reduction in ductility, on bare samples.
- Higher losses (strength/ductility) on embedded bars for same mass loss with bare.
- Development of pit depth measurement procedure, using advance imaging analysis.
- Pits significance analysis indicated more severe pitting corrosion on embedded bars.

ARTICLE INFO

Article history:
Received 6 April 2012
Received in revised form 13 July 2012
Accepted 23 July 2012

Keywords:
Chloride-induced corrosion
Mechanical properties
Ductility
Pit depth

ABSTRACT

In the current study the effects of chloride-induced corrosion, in terms of mechanical properties and pit depths, are evaluated on B500c steel bars embedded in concrete (embedded samples) and directly exposed (bare samples), immersed in a salt spray chamber. The results indicate that for the same level of mass loss, degradation of the "embedded" samples was found to be much more severe than that of the "bare samples", in terms of losses in yield strength and uniform elongation. Analysis of the statistical significance of the pit depth and area values measured, based on a methodology developed using advanced imaging analysis, indicate that degradation of the steel bars embedded in concrete produced a more severe pitting corrosion in terms of depth of pitting, compared to the steel samples directly exposed to the same corrosive medium, for the same (on average) mass loss.

1. Introduction

It is well known, that corrosion of steel reinforcement is one of the most important durability issues in reinforced concrete design [1,2]. It can be initiated due to chloride ingress in concrete or due to depassivation of the protective thin oxide film of the steel reinforcement (afforded by the high alkaline concrete environment) through the action of carbon dioxide from the atmosphere. Corrosion impairs not only the appearance of the structure, but also its strength and safety, with the subsequent reduction in the cross sectional area of the reinforcement and with the decrease of bond with the surrounding concrete [3,4]. In coastal regions (or marine environments) where high chloride concentrations are encountered, chloride-induced corrosion is the major source of environmental deterioration of reinforced concrete structures.

Trying to model corrosion level as a function of time, the representation of a bi-linear model (Fig. 1a) is usually used [5,6]. It is assumed that there is a period of time before chloride ions reach the reinforcement (initiation period), during which substances as water, chloride ions (and/or carbon dioxide) diffuses into concrete and reach the certain concentration necessary to trigger corrosion of the steel reinforcement. This threshold of chloride ions depends on a number of factors (type of binder, C_3A content and aggregate, moisture level, air content of concrete, ratio of chloride to the hydroxyl ion) [5,7]. In general when the chloride concentration exceeds 0.4% by weight of cement (for chlorides cast into concrete) or 0.2% (for chlorides diffusing in) corrosion is observed [5,7,8].

Chlorides that reach the concrete surface, enter the pore system either by diffusion (in stationary pore water), or by capillary suction of the surface water in which they are dissolved (or by combination of both transport mechanisms) [1,6]. In the majority of papers, chloride transport in concrete is modeled using the Fick's second law of diffusion neglecting the chloride interaction with the solid phase [9]. However, it is widely proved that chlorides

* Corresponding author. Tel.: +30 2610 911571; fax: +30 2610 911570.
E-mail addresses: charrisa@mech.upatras.gr (C.A. Apostolopoulos), sdemis@upatras.gr (S. Demis), vgp@psp.org.gr (V.G. Papadakis).

0950-0618/$ - see front matter © 2012 Elsevier Ltd. All rights reserved.
http://dx.doi.org/10.1016/j.conbuildmat.2012.07.087

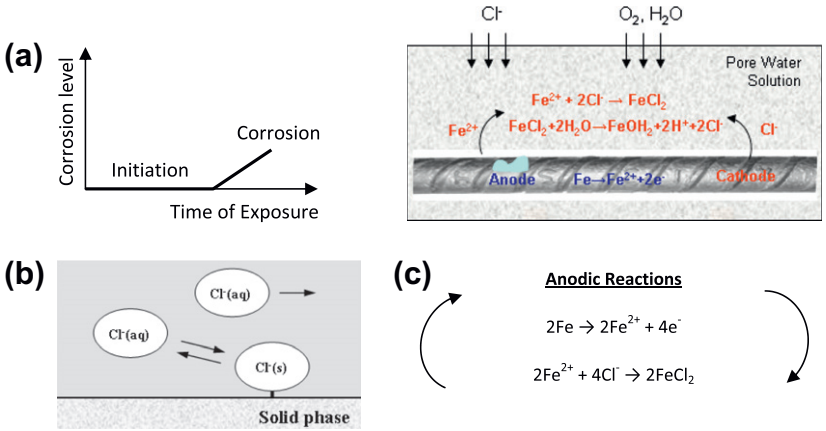

Fig. 1. Schematic representation of modeling aspects of chloride induced corrosion.

are bound from concrete components in a percentage of 30–60% depending on the cementitious materials' composition and content [5,6]. The interaction process (Fig. 1b) in general, includes binding of chlorides by cement hydration products, ionic interaction, lagging motion of cations and formation of an electrical double layer on the solid surface. Pereira and Hegedus [10] modeled chloride diffusion and reaction in fully saturated concrete as a Langmuirian equilibrium process coupled with Fickian diffusion. Papadakis et al. [11,12] extended this approach to more general conditions, offering a proven experimentally simpler solution. The physicochemical processes of Cl^- diffusion in the aqueous phase, their adsorption and binding in the solid phase of concrete and their desorption, are described by a non-linear partial differential equation [11,12], solution of which allows the calculation of the Cl^- bound in the solid phase and the estimation of the critical time for chloride-induced corrosion required for the total chloride concentration surrounding the reinforcement (located at a distance c from surface) to increase over the threshold for depassivation.

Chloride attack is distinct in that its primary action is the corrosion of steel reinforcement and only as a consequence of the corrosion process the surrounding concrete is damaged. The process leading to corrosion, and the factors affecting the corrosion of steel bars embedded in concrete (W/C ratio, type of binder, pore and capillary structure) have been widely investigated [1,7,8,13].

Corrosion propagation is taking place at a rate that depends on the availability of both oxygen and water at the cathode (Fig. 1c) [1,7,8,13]. However, even at low rates of O_2, severe pitting corrosion has been noticed [1,6]. It can be attributed to the fact that the anodic sites may be localized but the corresponding cathodic sites may be spread out over a wide area. In this way, as the corrosion product is discouraged from precipitation, and due to the existence of highly active and localized anodic sites, a severe pitting corrosion may occur without an earlier warning through visible signs at the surrounding concrete. This can lead to rapid loss of cross-section and critically reduce the load bearing capacity of the reinforced concrete member [14,15]. When cracks develop, the corrosion product will be deposited along the crack. By the time rust staining becomes apparent at the surface, the extent of reinforcement deterioration may be structurally significant.

Most of the available studies on the effects of corrosion refer on steel bars directly exposed to the corrosive environment (bare bars), usually under salt-spray exposure [16,17]. Aspects, as the subsequent mass loss, the depth and the density of the pits formed on its surface are usually evaluated [18,19]. What is however neglected to a great extend, even by the appropriate standards, is the evaluation of how the accumulated corrosion alters the mechanical properties of the steel bar. In the relevant Greek standard [20], for instance, (as well as in the other appropriate European National Standards), the ability of a steel bar for mechanical performance is considered as being unchanged during the entire lifetime of a reinforced concrete structure. It has been early recognized [19] that chloride induced corrosion, characterized by the continuous occurrence of pitted regions on the steel reinforcement, leads to substantial reductions in the bar cross-section. Such type of damage can have significant effects on strength [3,4,14,16,17,21–26] and ductility of reinforced concrete elements [19,23–25,27].

Given the above, apart a few valid efforts [4,14,16,17,19,21–27], investigations on the effects of corrosion on the mechanical performance of reinforcing steel bars remains rare. To this extend, the influence of accumulated corrosion damage of steel bars embedded in concrete on the reduction of bond strength between bar and concrete [3,4,19,21] has been investigated and assessed. ESEM observations on corroded steel bars (exposed to open atmosphere and sprayed daily with a 3.5 wt.% sodium chloride solution) [4] revealed that bond strength between steel rebar and concrete was reduced by 53%, for 122 days of exposure, due to the morphology and thickness of the rust layer on the steel surface. Furthermore, research results [25] on the effect of the degree of corrosion (expressed as the percent mass loss) on the mechanical properties of steel bars embedded in concrete slabs, indicated that a sudden failure of RC slabs in flexure was observed, for a mass loss of more than 13%. A decrease in the load bearing capacity of the steel reinforcement, due to the reduction of its cross sectional area (at the points were corrosion was concentrated) produced sudden failures without yielding, without the most desirable warning prior to failure of a structure.

Recently [22–24,26–28], it was demonstrated that steel bars subjected to corrosion (salt-spray) may suffer a relatively modest loss of strength but a significant loss of ductility. In general, in spite of research results available [29] were a correlation factor between natural corrosion and accelerated salt spray corrosion was estimated (in terms of corrosion attack rate and mass loss), there is not yet a widely accepted correlation of these results with those derived from bars embedded in concrete and exposed in a normal corrosive environment. Hence, additional experimental investigation is required in order to clarify the nature of the correlation of corrosion on bare and on embedded steel bars. Such is the aim of this study, where the effects of chloride induced corrosion on the tensile behavior of B500c reinforcing steel bars are investigated for samples exposed directly (noted as "bare") and embedded in concrete (noted as "embedded") under accelerated salt-spray exposure. Furthermore, the tensile properties of the corroded material were compared against the requirements set in the

standards for involving steels in reinforced concrete structures. It is hoped that the present approach will further shed some light on the interpretation of the mechanisms of chloride-induced corrosion in concrete structures.

2. Experimental methodology

Tensile testing samples of B500c bars (of 8 mm in diameter) were exposed directly and embedded in concrete cylinders, to a chloride rich environment (salt-spray). Each bar was cut to the tensile testing length of 460 mm, according to ISO/FDIS 15630-1 [30]. The 100 mm gauge length, according to [30], was marked on each specimen and its total length and mass were recorded before testing.

Prior to tensile testing, the specimens (directly exposed to the corrosive medium) were inserted in a laboratory salt-spray exposure chamber, in accordance to the ASTM B117-94 specification [31], for a period of up to 120 days (Fig. 2). The ASTM B117 specification [31] covers every aspect of the apparatus configuration, procedure and conditions required to create and maintain a salt spray (fog) testing environment. The selection of such a procedure for corroding the specimens, relies on the fact that the salt spray environment lies qualitatively closer to the natural coastal (rich in chlorides) conditions than any other accelerated laboratory corrosion test. In principle, the testing apparatus consists of a closed chamber in which a salted solution atomized by means of a nozzle, produces a corrosive environment of dense saline fog. In this particular study a special apparatus, model SF 450 (made by Cand W. Specialist Equipment Ltd.) was used. The salt solution was prepared by dissolving 5 parts by mass of sodium chloride (NaCl) into 95 parts of distilled water (pH range 6.5–7.2). The temperature inside the salt spray chamber was maintained at 35 °C (+1.1–1.7) °C.

As far as the embedded in concrete steel bars is concerned, cylindrical plastic tubes, were used as concrete molds, with an internal diameter of 32 mm and a total height of 340 mm. The steel bars were placed in the molds prior to concrete casting and were held in position using specific grips. A CEM IV (according to EN-197 [32]) cement type and crushed sand (and other fine aggregate) were used in the cement mix giving a water/cement (W/C) and aggregate/cement (A/C) ratios of 0.5 and 3, respectively. To increase the workability of the mix a certain type of superplasticizer (0.4% of cement weight) was used. The tubes were filled with concrete and vibrated for 20 s on a vibration table. After 24 h the molds were stripped and the concrete/steel specimens were immersed in lime-saturated water at 20 °C, for 28 days. Following this initial curing period, 10 specimens were placed in the laboratory salt spray exposure chamber for 1 year. It should be noted that since the primary aim of this particular study is to evaluate (and correlate) the nature of the corrosion damage on bare and on embedded steel bars, time of exposure is not a factor of comparison. Given the fact the corrosion rate in concrete is much slower than when the bars are directly exposed to the corrosive medium, a longer exposure period for the former (than in the case of the directly exposed bars) was selected. At the end of the exposure time the surrounding concrete was crushed and the corroded steel bars were removed for tensile testing.

At different time intervals tensile testing took place. At each testing date specimens were removed from the salt spray chamber, washed with clean running water to remove any salt deposits from their surfaces and air-dried. The corrosion products were removed from the surface of the specimen by means of a brittle brush, according to ASTM G1 specification [33]. The specimens were then weighed and the mass loss due to corrosion exposure was calculated as:

$$\Delta m = \frac{m_0 - m_c}{m_0} \times 100\% \quad (1)$$

where m_0 is the mass of uncorroded specimens and m_c the reduced mass of the corroded specimen.

The tensile tests were performed according to the ISO/FDIS 15630-1 specification [30], using a servo-hydraulic MTS 250KN machine with a constant elongation rate of 2 mm/min. The mechanical properties, yield strength R_p, ultimate strength R_u, and uniform elongation A_{gt}, were determined. It should be noted that A_{gt} was measured according to the manual method described in the relevant standard [30] (on a gauge length of 100 mm, at a distance of 50 mm away from the fracture). In addition, as presented in Section 4, measurement and statistical analysis of the pits formed on the surface of the bars took place, based on a methodology developed using advanced imaging analysis.

3. Results

The results of the mechanical testing of samples exposed directly to the corrosive medium (bare samples) are given in Table 1. It can be seen that mass loss is almost linear with time of exposure (Fig. 3). In terms of strength, the nominal values of yield strength (R_p) and ultimate tensile strength (R_u) were calculated (as the ratio of the corresponding load capacity, divided by the initial, uncorroded cross section of the steel bars). The latter was done according to the corresponding standards, in which the mass, and therefore the cross sectional area of the specimens are considered to be constant over time, neglecting in this way the reduction of the cross section due to the effects of corrosion. According to the results, for an observed final mass loss of 13.55%, yield strength was reduced by 31.4%, compared to a 22.9% reduction of ultimate tensile strength, after 120 days of exposure in the salt-spray chamber (Fig. 4). What strikes the most, from the graphic representation of the results (Fig. 3), is the percentage reduction of the uniform elongation. It increases considerably with time of exposure in salt spray, from 19.2% to 66.2% (at 30 and 120 days of exposure, respectively) and it is much higher than that of the corresponding mass and strength loss (percentage reductions).

It should be mentioned at this point that, the modest loss of strength and more important, the significant loss of ductility observed on the steel samples exposed directly to the corrosive medium, is in accordance with results from other studies in the literature [14,24,26–28]. Tensile tests on different types and bar sizes of corroded reinforcement [14,28] indicated that after a certain level of mass loss the influence of corrosion on elongation is far greater than its influence on tensile strength. Such a trend has been attributed to the pitting result of the chloride-induced corrosion and the corresponding local section loss [14,24] on the bar. Observations of the fracture section after tensile tests [28] concluded that fracture starts from the point of pitting leading to brittle fracture with low strength and less elongation.

As far as the embedded in concrete steel samples is concerned (exposed to the corrosive medium for 1 year) a mass loss (average) of 2.41% was observed (Table 2). On average, a yield strength of 490.26 MPa was produced (reduced by 21.15% compared to the un-corroded specimens), lower than the limit of 500 MPa imposed in the standards for using steels in reinforced concrete structures. In terms of uniform elongation an average value of 7.39% was observed, again lower than the 7.5% limit set in the relevant standards, reduced by 28.5% compared to the un-corroded specimens.

Using linear interpolation on the mass loss data of the bare samples, it was found that the 2.41% mass loss observed on the embedded samples, corresponds on the bare samples to 18 days of exposure to accelerated salt-spray. Based on the results of the tensile testing of the bare samples (Table 1), using linear interpolation,

Fig. 2. Salt spray exposure chamber, preparation and testing of steel samples.

Table 1
Mass loss, strength and ductility properties versus time of exposure for bare steel bars (B500c) exposed to chloride-induced corrosive environment.

Time (days)	Mass loss Δm (%)	Yield stress nominal R_p (MPa)	EC 2 limit of $\geqslant$500 MPa	Ultimate stress nominal R_u (MPa)	Uniform elongation A_{gt} (%)	EC 2 limit of $\geqslant$7.5%
0	0	621.77	√	734.99	10.31	√
10	1.33	597.54	√	712.11	9.95	√
20	2.67	575.43	√	687.37	9.25	√
30	3.03	564.21	√	684.43	8.33	√
45	5.15	539.42	√	658.64	6.57	–
60	6.55	525.45	√	639.99	5.79	–
90	9.89	488.30	–	597.69	4.51	–
120	13.55	426.07	–	565.39	3.36	–

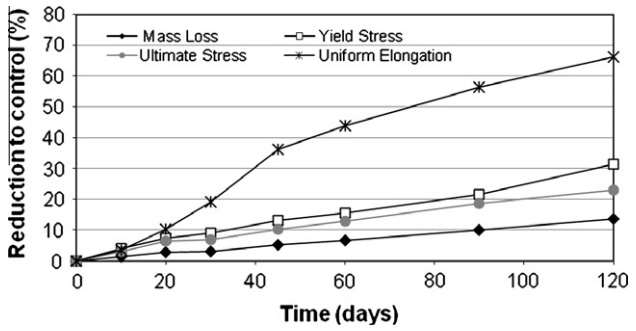

Fig. 3. Effect of the time of exposure on the loss of mass and mechanical performance of embedded steel bars.

the values of yield strength and uniform elongation for 18 days exposure to salt-spray (hence 2.41% mass loss) were calculated as 579.72 MPa and 9.39% respectively (Fig. 4). From these results it is obvious that, in the case of bare bars, 2.41% of mass loss is still acceptable, i.e. yield strength and uniform elongation do not drop below limits.

Comparing the effects of the corrosive medium (salt-spray exposure) for the same level of mass loss (2.41%), on the ductility properties (yield strength and uniform elongation) of the bare and embedded samples (Fig. 5), it becomes evident that higher losses are observed when the steel bars are embedded in concrete (embedded samples). Such an observation has also been derived in another investigation of accelerated corrosion of embedded and bare steel bars of different types and sizes [27]. More specific in the current study, 21.15% and 28.32% reductions were observed on the yield strength and uniform elongation respectively of the embedded samples (exposed to salt-spray for 1 year), compared to the corresponding reductions of 6.76% and 8.92% of the bare bars (exposed in the corrosive medium for 18 days).

This important finding might indicate that the corrosion process on the embedded steel bars is more severe than on bare bars, probably due to a deeper or more extended pitting. In general, corrosion damage on embedded in concrete steel bars is in favor of higher stress concentrations and to a more severe environment due to the surrounding concrete cover, resulting in this way to a higher level of damage even for the same degree of mass loss. Comparing the general image of deterioration observed on the two different set of samples exposed to the corrosive medium (bare, embedded

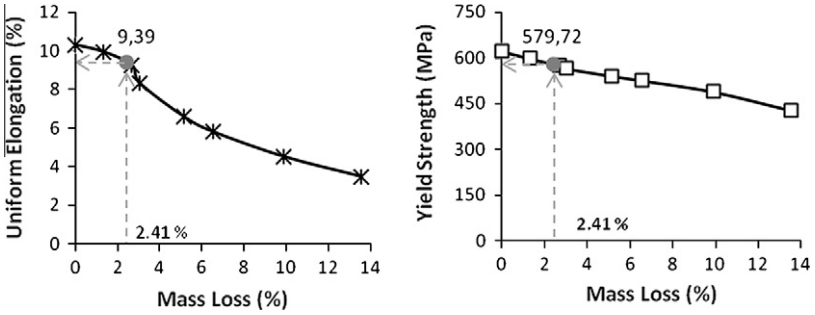

Fig. 4. Linear interpolation for a 2.41% mass loss on the properties of bare samples.

Table 2
Mass loss, strength and ductility properties versus time of exposure, of embedded steel bars.

Sample	Mass loss Δm (%)	Yield stress R_p (MPa)	EC 2 limit of $\geqslant$500 MPa	Uniform elongation A_{gt} (%)	EC 2 limit of $\geqslant$7.5%
1	0.75	448.52	–	6.30	–
2	3.58	520.09	√	8.75	√
3	2.43	467.97	–	5.56	–
4	4.20	452.43	–	5.00	–
5	1.96	494.89	–	8.75	√
6	1.32	534.66	√	10.0	√
7	1.30	513.92	√	10.0	√
8	2.09	503.29	√	7.50	√
9	3.48	467.81	–	5.00	–
10	2.97	499.01	–	7.00	–
Average	2.41	490.26	–	7.39	–
St. dev.	1.13	29.56		1.93	

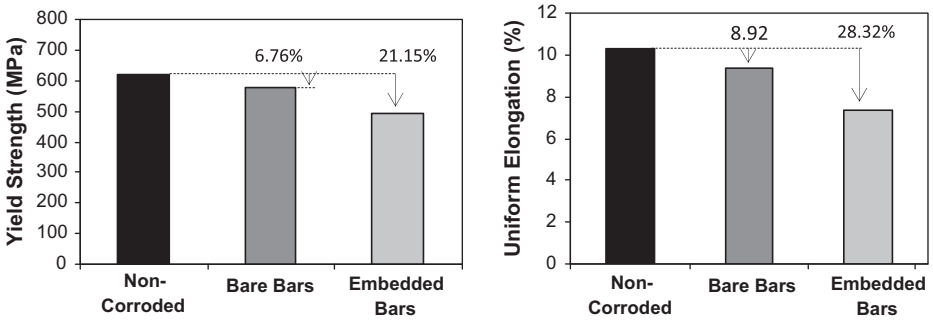

Fig. 5. Comparison of degradation of the ductility properties, (a) yield strength and (b) uniform elongation, for bare and embedded bars, for the same level of mass loss (2.41%).

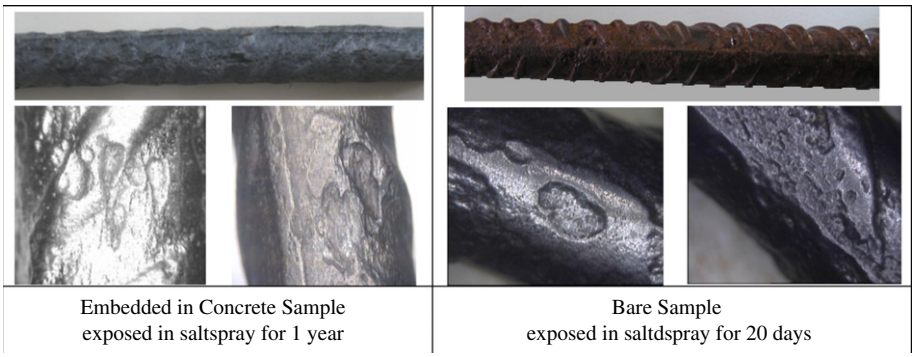

Fig. 6. Effects of corrosion on the surface of embedded and bare samples.

samples for a similar level of mass loss) a first observation that can be made is that a not so different pattern of corrosion is observed (Fig. 6). Corrosion attack initiated at the rib roots and advanced towards the area between the ribs. Pitting corrosion is evident on both types of samples. The question is to what extend.

4. Pit depth analysis

To further elaborate on the previous observation, identification, measurement and statistical analysis of the pits formed on the surface of the bars took place. Pits were identified along the length of the bars (away from the grips, to avoid damage through wedging effects), on samples embedded in concrete and on samples directly exposed to salt-spray for 10 and 20 days (the latter was deemed necessary, since the 2.41% mass loss of the embedded samples was found to correspond to 18 days of exposure to salt-spray).

Stereoscopical images taken at the locations of the pits (using a $\times$35 magnification lens) were converted to 8-bit gray-scale and normalized using special filter algorithms in order to bring the resolution and the lighting conditions (between the photos taken at different testing dates) to a common level. On each pit several pit depth measurements were taken (Fig. 7) in order to calculate the average pit depth (in addition to the maximum and the minimum pit depth). Based on the individual values according to the gray-scale intensity (255 shades of gray) of the stereoscopical photos taken, three-dimensional (3D) surface plots of representative pits were also determined to obtain a visual representation of the size of pits measured. In addition, the area of each pit was calculated automatically using imaging software analysis.

Overall, a 18.3% difference was observed between the average pit depth values of the steel samples embedded in concrete (0.477 mm) and those exposed directly in the corrosive medium for 20 days (0.39 mm). The difference on the average maximum depth observed was found to be 21.5% (Table 3).

In general the embedded samples produced larger pit depths (Fig. 8b). Comparing the frequency distribution of the pit depths measured, meaning the number of pit depths identified within a particular depth range, it can be seen that (Fig. 8a) on the embedded samples the majority of the pit depths identified are in the 0.6–0.8 mm range (with high occurrences of pit depths of 0.8 mm and above). On the contrary on the bare samples exposed for 20 days, the vast majority of pit depths identified lays in the region of 0.4–0.6 mm.

In order to get a visual representation of the size of the pit which its depth was estimated, three dimensional (3D) surface plots of each pit were derived based on the gray-scale intensity of the converted to gray-scale pit images. This is a technique which has been used in other studies [34] on the digital reconstruction of corroded concrete surfaces. Each converted to gray-scale image was transformed into a single matrix in which each pixel value represented shades of black and white (low values were the darkest, in total 255 shades of gray). Based on pixel information contours of shadows were used to form the 3D features of each pit. The depth was visualized as a difference in pixel units (gray scale resolution), as it is shown in Fig. 9. Bearing in mind that this attempt is a visualization, the difference on the pit depths identified on the embedded and the bare samples is evident.

In terms of area measured, the values obtained from the embedded and the 20 days bare samples, although on average they produced a difference of 11.4%, the majority of the measurements obtained, apart of a few exceptions (indicated with a rectangular area in Fig. 10b) does not seem to differ substantially. However, the situation compared to the 10 days bare sample is different.

Trying to further elaborate on the differences observed on the measured values of pit depth and area, statistical analysis took

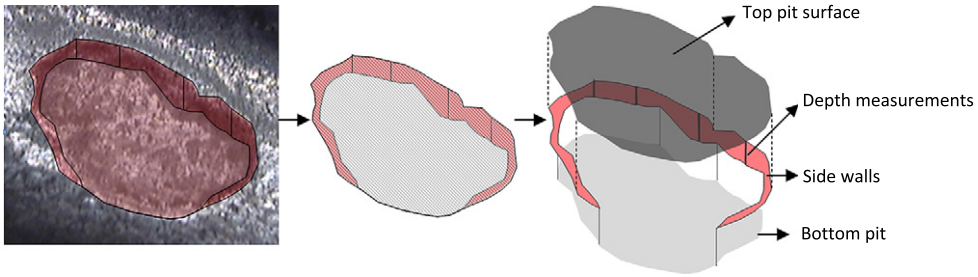

Fig. 7. Schematic representation of pit depth and area measurement.

Table 3
Average values of pit depths and area measured.

		Bare 10 days	Embedded	Bare 20 days	Differences 20 days-embedded (%)
Pit depth (mm)	Minimum (d_{min})	0.233	0.367	0.309	15.7
	Average (d_{avg})	0.277	0.477	0.390	18.3
	Maximum (d_{max})	0.325	0.599	0.470	21.5
Area (mm^2)	Minimum (A_{min})	0.703	0.649	0.758	–
	Average (A_{avg})	2.424	7.146	6.331	11.4
	Maximum (A_{max})	7.642	29.838	24.704	–

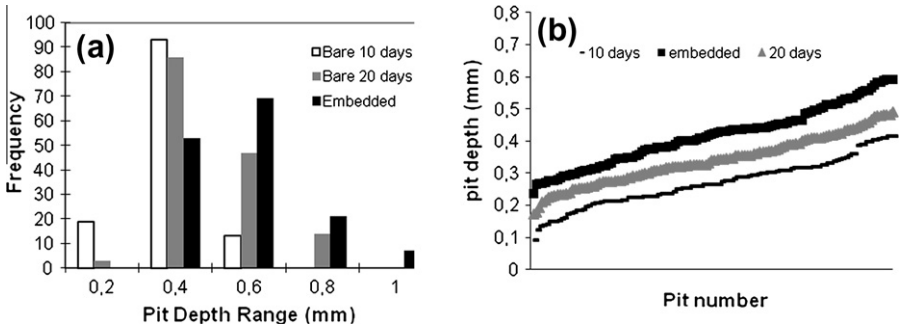

Fig. 8. Frequency (a) and distribution (b) of the average pit depth values.

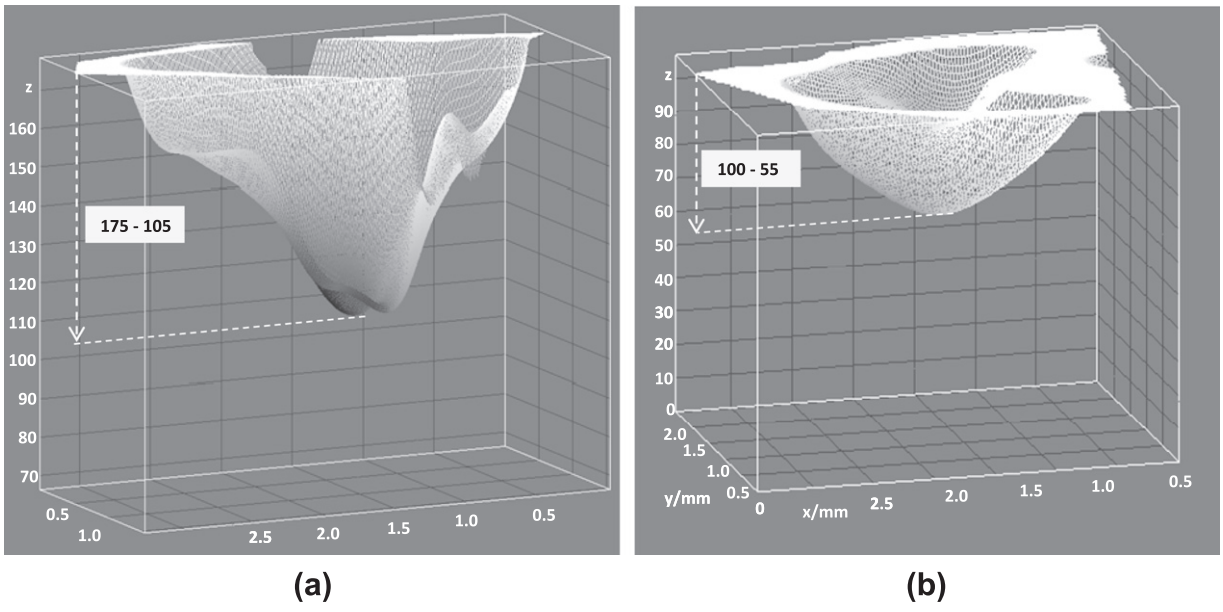

Fig. 9. 3D surface plots of (a) embedded and (b) bare 20 days samples (vertical axis in pixel units, horizontal axes in mm).

place in order to establish if the observed differences (mainly between the embedded and the 20 days samples) are statistically significant or not. The results of such an analysis (based on a total of 425 individual pit depth measurements, for all the samples

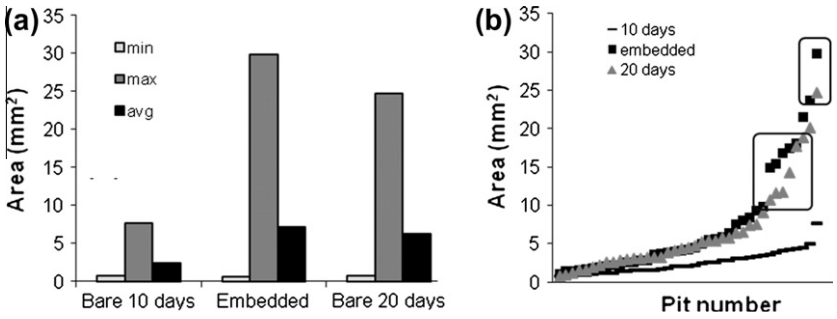

Fig. 10. Distribution and scattering of the area values.

Table 4
Statistical significance of differences observed.

	Pit depth			Area	
	d_{avg} Embedded/bare 20 days	d_{max} Embedded/bare 20 days	d_{min} Embedded/bare 20 days	Embedded/bare 20 days	Embedded/bare 10 days
t	3.521	3.731	2.981	0.565	4.131
$t_{critical\ (one\text{-}side)}$	1.664	1.664	1.664	1.665	1.664
$t_{critical\ (two\text{-}sided)}$	1.991	1.991	1.991	1.992	1.991
$P_{one\text{-}side}$	0.000361	0.000179	0.00191	0.287	4.507 E−05
$P_{two\text{-}sided}$	0.000722	0.000359	0.00383	0.574	9.014 E−05
a (Level of significance)	0.05	0.05	0.05	0.05	0.05
Statistically significant difference	YES $t > t_{critical}$, $P < 0.05$	YES $t > t_{critical}$, $P < 0.05$	YES $t > t_{critical}$, $P < 0.05$	NO $t < t_{critical}$, $P > 0.05$	YES $t > t_{critical}$, $P < 0.05$

involved) are given in Table 4. As it was expected, based on the observations previously mentioned, the pit depth values measured of the embedded and the 20 days bare samples have a statistically significant difference (in terms of average, minimum and maximum pit depth observed) but not their corresponding areas. Of course, the area measurements between the embedded and the 10 days bare sample have a statistically significant difference.

Hence, according to the measured pit depths and area values, the frequency trends observed and the results of their statistical significance it is concluded that, the degradation of the steel bars embedded in concrete produced a more severe pitting corrosion in terms of depth of pitting, compared to the steel samples directly expose for 10 and 20 days, to the same corrosive medium.

5. Discussion

Such an observation (and a behavior) can be explained due the level of influence the concrete environment entails on the electrochemical nature of the chloride induced corrosion process. It can be safely stated that corrosion kinetics (in terms of ion mobility and their interactions as defined on the various phases of the corrosion process) are clearly different for steel embedded in concrete compared with samples in solution (being NaCl, or simulated concrete pore water solution) [1].

In concrete, the local breakdown of the passivity of steel reinforcement (afforded by the high pH of the concrete environment) can be influenced (and accelerated) by a number of factors, including Heterogeneities in the surface of the steel, defects on the steel–concrete interface [15], local differences in the electrolyte, due to the heterogeneous nature of concrete, fluctuations in pH (near the reinforcement) [35] and level of moisture (which tends to be retained well within the concrete mass, irrespective of external fluctuations).

Pitting attacks have been found to be partially attributed to localized steel–concrete interface imperfections [15]. In general chloride induced corrosion in concrete tends to create localized active zones of dissolving metal and passive areas, known as the macro-cell effect [1]. Macrocells normally occur, when the chloride content of the concrete is not constantly high, but unevenly distributed along the steel surface. They consist of anodically acting regions, normally where the critical chloride content has been reached, and large cathodes being next to the anodes (usually observed in steel samples exposed in corrosive solutions [36], or at some distance from anodes (as in the case of steel embedded in concrete [37,38]). Normally the loss of steel in the anodically acting surface areas is much higher in the case of macrocell corrosion, because large cathodically acting areas support the local iron removal. Measurements on cracked reinforced concrete specimens verified that chloride induced steel corrosion involves the formation of macro-corrosion cells [37].

Similar levels of the severity and mode of chloride induced deterioration of steel bars in concrete, observed in this study, have also been found by other researchers. Localized pitting corrosion was identified as the predominant corrosion pattern in reinforced concrete structures [39,40], even after 14 years of natural exposure to a chloride reach environment [15]. Even though results vary, the maximum pit depths observed [39–41] are 4–8 times higher than the average pit depths (in other words maximum/average pit depth ratio), illustrating the severity of a concrete chloride reach environment (for example, an average pit depth of 0.38 mm was observed after 6 years immersion of an embedded in concrete 8 mm steel bar, in sea water [39] (reaching a maximum of 1.72 mm).

6. Conclusions

The effects of the chloride-induced corrosion in terms of mechanical properties, on B500c steel samples exposed directly and as embedded in concrete to salt spray were evaluated and presented in the current study. Overall, direct exposure to salt

spray of B500c steel bars produced a moderate loss of strength but a significant reduction of ductility (an observation in accordance with other research attempts). By comparing the strength and ductility properties (yield strength and uniform elongation) of the bare (directly exposed) and embedded samples, for the same level of mass loss (2.41%), it became evident that higher losses were observed when the steel bars were embedded in concrete. To further reinforce this observation, analysis of the pitting morphology of the samples took place. Using advanced imaging analysis a methodology was developed, to reliable estimate the average pit depth and its area. Overall, based on the research findings and the corresponding analysis as it was described in this study, it can be concluded that

- Analysis of the statistical significance of the pit depth and area values measured, indicate that the exposure of the embedded samples and the bare bars (for 20 days in salt-spray chamber) have a statistically significant difference in terms of pit depths but not in terms of area.
- In other words, degradation of the steel bars embedded in concrete produced a more severe pitting corrosion in terms of depth of pitting, compared to the steel samples directly exposed to the same corrosive medium, for the same (on average) mass loss.

Conclusions, also observed in other studies [14,26–28,39–41], explained due the level of influence the concrete environment entails on the electrochemical nature of the chloride induced corrosion process.

References

[1] Page CL, Tredaway KWJ. Aspects of the electrochemistry of steel in concrete. Nature 1982;297:109–15.
[2] Gonzalez JA, Felifi S, Rodffguez P, Ramlrez E, Alonso C, Andrade C. Some questions on the corrosion of steel in concrete – Part 1: when, how and how much steel corrodes. Mater Struct 1996;29:40–6.
[3] Demis S, Pilakoutas K, Apostolopoulos CA. Effect of corrosion on bond strength of steel and non-metallic reinforcement. Mater Corros 2010;61(4):328–31.
[4] Batis G, Rakanta E. Corrosion of steel reinforcement due to atmospheric pollution. Cement Concr Compos 2005;27:269–75.
[5] Angst U, Elsener B, Larsen CK, Vennesland O. Critical chloride content in reinforced concrete—a review. Cem Concr Res 2009;39:1122–38.
[6] Ozbolt J, Balabanic G, Periskic G, Kuster M. Modelling the effect of damage on transport processes in concrete. Constr Build Mater 2010;24:1638–48.
[7] Papadakis VG. Effect of supplementary cementing materials on concrete resistance against carbonation and chloride ingress. Cem Concr Res 2000;30:291–8.
[8] Shi X, Xie N, Fortune K, Gong J. Durability of steel reinforced concrete in chloride environments: an overview. Constr Build Mater 2012;30:125–38.
[9] Richardson MG. Fundamentals of durable reinforced concrete. London: Spon Press; 2002.
[10] Pereira CJ, Hegedus LL. Diffusion and reaction of chloride ions in porous concrete. In: Proceedings of the 8th international symposium of chemical reaction engineering, Edinburgh, Scotland; 1984.
[11] Papadakis VG, Fardis MN, Vayenas CG. Physicochemical processes and mathematical modeling of concrete chlorination. Chem Eng Sci 1996;51:505.
[12] Papadakis VG, Roumeliotis AP, Fardis MN, Vayenas CG. Mathematical modeling of chloride effect on concrete durability and protection measures. In: Dhir RK, jones MR, editors. Proceedings of international congress: concrete in the service of mankind, concrete repair, rehabilitation and protection. London: Dundee, Scotland; E. & F.N. SPON; 1996. p. 165–74.
[13] Neville A. Chloride attack of reinforced concrete: an overview. Mater Struct 1995;28:63.
[14] Cobo A, Moreno E, Canovas MF. Mechanical properties variation of B500SD high ductility reinforcement regarding its corrosion degree. Materiales de Construccion 2011;61(304):517–32.
[15] Zhang R, Castel A, Francois R. The corrosion pattern of reinforcement and its influence on serviceability of reinforced concrete members in chloride environment. Cem Concr Res 2009;39:1077–86.
[16] Apostolopoulos ChA, Papadopoulos M, Pantelakis S. Tensile behaviour of corroded reinforcing steel bars BSt 500s. Constr Build Mater 2006;20:782–9.
[17] Apostolopoulos ChA. Mechanical behavior of corroded reinforcing steel bars S500s tempcore under low cycle fatigue. Constr Build Mater 2007;21:1447–56.
[18] Borgard B, Warren C, Somayaji R, Heidersbach R. Mechanisms of corrosion of steel in concrete. ASTM STP 1065, Philadelphia; 1990.
[19] Capozucca R. Damage to reinforcement concrete due to reinforcement corrosion. Constr Build Mater 1995;9:295.
[20] Hellenic Regulation for the Technology of Steel in Reinforced Concrete (KTX-2008). Government Gazette Issue 2113/B/13.10.2008. Hellenic Ministry of Environment, Physical Planning and, Public Works; 2008.
[21] Fang C, Lungren K, Chen L, Zhu C. Corrosion influence on bond in reinforced concrete. Cem Concr Res 2004;34:2159.
[22] Apostolopoulos CA. The influence of corrosion and cross-section diameter on the mechanical properties of B500c steel. J Mater Eng Perform 2009;18:190.
[23] Apostolopoulos CA, Papadakis VG. Consequences of steel corrosion on the ductility properties of reinforcement bar. Constr Build Mater 2008;22:2316.
[24] Cairns J, Plizzari GA, Du Y, Law DW, Frnazoni C. Mechanical properties of corrosion-damaged reinforcement. ACI Mater J 2005;102(4):256–64.
[25] Almusallam AA. Effect of degree of corrosion on the properties of reinforcing steel bars. Constr Build Mater 2001;15(8):361–8.
[26] Du YG, Clark LA, Chan AHC. Residual capacity of corroded reinforcing bars. Mag Concr Res 2005;57(3):135–47.
[27] Du YG, Clark LA, Chan AHC. Effect of corrosion on ductility of reinforcing bars. Mag Concr Res 2005;57(7):407–19.
[28] Lee HS, Cho YS. Evaluation of the mechanical properties of steel reinforcement embedded in concrete specimen as a function of the degree of reinforcement corrosion. Int J Fract 2009;157:81–8.
[29] Papadopoulos MP, Apostolopoulos CA, Zervaki AD, Haidemenopoulos GN. Corrosion of exposed rebars, associated mechanical degradation and correlation with accelerated corrosion tests. Constr Build Mater 2011;25(8):3367–74.
[30] ISO/FDIS 15630-1. International Standard. Steel for the reinforcement and prestressing of concrete – test methods. Part 1: reinforcing bars, wire rod and wire; 2002.
[31] ASTM Standard B117. Standard Practice for Operating Slat Spray (Fog) Apparatus. ASTM International, West Conshohocken, PA; 2003, doi: 10.1520/B0117-97; 1997.
[32] CEN EN 197-1. European standard for cement – Part 1: composition, specifications and conformity criteria for common cements, European Committee for Standardization, Brusells; 2000.
[33] ASTM Standard G1. Standard practice for preparing, cleaning, and evaluating corrosion test specimens, ASTM International, West Conshohocken, PA; 2011.
[34] Gutierrez-Padilla MGD, Bielefeldt A, Ovtchinnikovb S, Pellegrinoa J, Silversteina J. Simple scanner-based image analysis for corrosion testing: Concrete application. Journal of materials processing technology 2009;209:51–7.
[35] Junga WY, Yoonb YS, Sohn YM. Predicting the remaining service life of land concrete by steel corrosion. Cem Concr Res 2003;33:663–77.
[36] Zhang F, Pan J, Lin C. Localized corrosion behaviour of reinforcement steel in simulated concrete pore solution. Corros Sci 2009;51:2130–8.
[37] Raupach M. Chloride-induced macrocell corrosion of steel in concrete – theoretical background and practical consequences. Constr Build Mater 1996;10(5):329–38.
[38] Angsta U, Elsenerb B, Larsena CK, Vennesland O. Chloride induced reinforcement corrosion: rate limiting step of early pitting corrosion. Electrochim Acta 2011;56:5877–89.
[39] Gonzalez JA, Andrade C, Alonso C, Feliu S. Comparison of rates of general corrosion and maximum pitting penetration on concrete embedded steel reinforcement. Cem Concr Res 1995;25(2):257–64.
[40] Vidal T, Castel A, Francois R. Corrosion process and structural performance of a 17 year old reinforced concrete beam stored in chloride environment. Cem Concr Res 2007;37:1551–61.
[41] Stewart MG, Al-Harthy A. Pitting corrosion and structural reliability of corroding RC structures: experimental data and probabilistic analysis. Reliab Eng Sys Saf 2008;93:373–82.